Weakly Conjugated Bacteriochlorin-Bacteriochlorin Dyad: Synthesis and Photophysical Properties

Zhanqian Yu,[†] Brian Uthe,[‡] Rachel Gelfand, [‡] Matthew Pelton, [†‡*] Marcin Ptaszek[†*]

†Department of Chemistry and Biochemistry

‡Department of Physics

University of Maryland, Baltimore County

1000 Hilltop Circle

Baltimore, MD 21250

**corresponding authors*

mptaszek@umbc.edu (M. Ptaszek)

mpelton@umbc.edu (M. Pelton)

Received and Accepted dates:

Abstract

Dyads containing two near-infrared absorbing and emitting bacteriochlorins with distinct spectral properties have been prepared and characterized by absorption, emission, and transient-absorption spectroscopies. The dyads exhibit ultrafast (~3 ps) energy transfer from the bacteriochlorin with the higher-energy S_1 state to the bacteriochlorin emitting at the longer wavelength. The dyads exhibit strong fluorescence and relatively long excited state lifetimes (~ 4 ns) in both non-polar and polar solvents, which indicates negligible photoinduced electron transfer between the two bacteriochlorins in the dyads. These dyads are thus attractive for the development of light-harvesting arrays and fluorophores for *in vivo* bioimaging.

Keywords: bacteriochlorins, near-IR, fluorophores, energy transfer, light harvesting

INTRODUCTION

Multipigment energy transfer arrays have received considerable interest due to their potential applications as fluorescent probes [1-3], fluorophores for *in vivo* imaging [2,3], models of light-harvesting antennas [4-6], and photosynthetic reaction centers [5,6]. Among others, energy arrays composed of hydroporphyrins are of particular interest [7-10]. Hydroporphyrins are synthetic analogs of photosynthetic pigments, thus their arrays are important models to study energy and electron transfer processes in natural photosynthesis [7-10]. Moreover, hydroporphyrins exhibit deep-red and near-IR absorption and emission, thus their arrays are promising platforms for development of advanced fluorescence probes for *in vivo* imaging [11-13]. Among hydroporphyrins, bacteriochlorins are of particular interest, since their strong near-IR (> 700 nm) absorption and emission render them promising chromophores for a variety of photonic applications [8,14]. For example, application of bacteriochlorin arrays in artificial photosynthesis should be highly beneficial since a large fraction of solar radiation falls in the near-IR spectral window [15]. Bacteriochlorin-bacteriochlorin arrays are also potentially attractive candidates for fluorophores for *in vivo* multicolor imaging. A properly designed dyad architecture should allow for the development of a series of fluorophores with common near-IR excitation and tunable near-IR emission [11,12,16]. The latter property is possible due to the narrow emission band and the excellent tunability of emission wavelength for bacteriochlorin [17].

The number of covalent arrays containing bacteriochlorins significantly increased recently, and examples of chlorin-bacteriochlorin [11,12,18-24], bacteriochlorin-bacteriochlorin [25-30], bacterochlorin-BODIPY [12,31-33] bacteriochlorin-cyanine [34], bacteriochlorin-peryleneimide [35], bacteriochlorin-naphthaleneimide [36], and bacteriochlorin-diketopyrrolopyrrole [37,38] arrays have been reported. However, there is only handful of reports of bacteriochlorin-bacteriochlorin arrays, composed of weakly electronically interacting pigments [25,28,29]. Such dyads would be a useful model system for studying energy transfer dynamics for photosynthetic pigments. The

extensive investigation of porphyrin-porphyrin as well as chlorin-chlorin and chlorin-bacteriochlorin arrays has revealed important differences in the predominant mechanisms of energy transfer among arrays composed of a different tetrapyrrolic macrocycles. In porphyrin-porphyrin arrays, the through-bond energy transfer mechanism is dominant, at least for arrays where porphyrin subunits are connected by a conjugated linker [39], whereas in chlorin-chlorin [40] and chlorin-bacteriochlorin [21] arrays the Förster (through-space) mechanism accounts for at least 75% of energy transfer. The more prominent contribution of Förster energy transfer in the hydropoprhyrin arrays stems primarily from the greater oscillator strength of their longest-wavelength Q_y bands compared to porphyrins. The rate, efficiency, and mechanism of energy transfer in bacteriochlorin arrays are of great importance in the view of their potential application in light-harvesting antenna.

Another important aspect of baceriochlorin-array photophysics is the potential occurrence of photoinduced electron transfer (PET). For chlorin-bacteriochlorin [22,23] and strongly electronically interacting bacteriochlorin-bacteriochlorin dyads [26-29], a significant reduction of both excited state lifetime and fluorescence quantum yield was reported in solvents of high dielectric constants, which was attributed to PET between dyad components. The directionality of PET depends on the exact redox potential of the array components [22]. For application of bacteriochlorin arrays in artificial photosynthesis, efficient PET leading to long-lived charge separated state would be highly beneficial, allowing the development of systems combining light harvesting and charge separation [5]. On the other hand, PET may have a detrimental effect on application of bacteriochlorin arrays as fluorophores for *in vivo* imaging, since it would lead to significant quenching of fluorescence in polar microenvironments.

Here, we describe synthesis and photophysical characterization of a weakly conjugated bacteriochlorin-bacteriochlorin dyad BC1-BC2 (Chart 1), composed of two bacteriochlorins with distinctive absorption properties. The absorption features are achieved by a different set of substituents installed on the periphery of macrocycles. In particular, we focus on dynamics of energy transfer and determination of a putative electron transfer between bacteriochlorin subunits in solvents with high dielectric constants. We also examined monomers BC1 and BC2 [16,41] (Chart 1) as benchmarks for bacteriochlorin donor and acceptor, respectively.

<Chart 1>

RESULTS AND DISCUSSION

Design and synthesis. The architecture of BC1-BC2 is inspired by chlorin-bacteriochlorin arrays, described previously [16]. Two bacteriochlorin subunits are connected by an amide linker. The linker fragments function also as auxochromes that tune absorption properties of both chromophores, i.e. aryl group installed at 15-position of BC1 subunit, and phentylethynyl, installed at 13 position of BC2.

Syntheses of BC1-BC2 as well as BC1 benchmark are outlined in Schemes 1-3. The key building blocks are 4-aminophenyl-substituted BC-NH_2 (Scheme 1) and 4-carobxylatephenylacetylene-substituted bacteriochlorin, prepared *in situ* by hydrolysis of previously reported ester BC2 [16,41] (Scheme 2). BC-NH_2 was prepared by

Suzuki reaction of **BC-Br** [42] and 4-(4,4,5,5-tetramethyl-1,3,2-dioxaborolan-2-yl)aniline **1** with 88% yield. Dyad **BC1-BC2** was synthesized in an analogous way as previously reported amide-linked chlorin-bacteriochlorin arrays (Scheme 2) [16]. Basic hydrolysis of **BC2** provides a corresponding carboxylic acid, which was then reacted with **BC-NH$_2$** in the presence of EDC·HCl and DMP in DMF. **BC1-BC2** was isolated with 81% yield. Benchmark **BC1** was obtained in Suzuki reaction of **BC-Br** with boronate 2, with 82% yield.

Both **BC1-BC2** and **BC1** were characterized by ^{1}H NMR and HRMS. In addition, BC1 was characterized by ^{13}C NMR (we were unable to obtain good quality ^{13}C NMR for **BC1-BC2**). Spectra are consistent with the proposed structures. In particular, ^{1}H NMR spectrum of **BC1-BC2** consists two sets of resonances from two distinctive bacteriochlorins.

<Scheme 1>

<Scheme 2>

<Scheme 3>

Absorption and emission properties. The absorption spectrum of **BC1-BC2** in toluene (Figure 1, Table 1)) consists of two distinctive Q_y bands, positioned at 713 nm and 760 nm, as well as two distinctive Q_x bands, positioned at 509 nm and 526 nm. The wavelengths for the maxima of the bands in the dyad match exactly the wavelengths of the corresponding bands in the benchmark monomers (Figure 2), which clearly indicates the weak electronic interactions between both bacteriochlorins. This is consistent with results for previously reported analogous chlorin-bacteriochlorin arrays [16]. Absorption spectra for **BC1-BC2** and the benchmark monomer are nearly indpendent of the solvent. It is interesting to note that the ratio of absorbance at the λ_{max} of Q_y bands of **BC1** and **BC2** components in dyad is 1.55.

Emission spectra (Figure 1, Table 1) of the dyad consist predominantly of an emission band centered at 762 nm, which corresponds to emission of the **BC2** component, while fluorescence of the **BC1** component is significantly reduced, regardless of the wavelength of excitation. Excitation spectra monitored at ~ 800 nm closely resemble the absorption spectrum of the dyad (Figure S1). These observations are fully consistent with an efficient energy transfer from the **BC1** component to the **BC2** subunit in dyad. Inspection of excitation spectra and comparison of fluorescence quantum yields (Φ_f) upon excitation at the Q_x band of the **BC1** and **BC2** components (see below) indicates that the efficiency of the energy transfer is greater than 95%.

Φ_f for the dyad in toluene matches that of the **BC2** benchmark (Table 1). In DMF, Φ_f is moderately quenched (~75% of that in toluene). The same is true for the fluorescence lifetime (τ_f), which in toluene matches that of benchmark monomer, whereas in more polar solvent (benzonitrile, PhCN) in reduced (~80% of that in toluene). The small quenching of fluorescence of the **BC1-BC2** dyad in polar solvent (compared to >10-fold quenching

observed, for example, in directly-linked strongly-conjugated bacteriochlorin dyads [23,24,27,28]) indicates that photoinduced electron transfer is inefficient in this weakly conjugated array.

<Figure 1>

<Figure 2>

<Table 1>

Kinetics of energy transfer. To get quantitative insight into the kinetics of energy transfer, femtosecond transient absorption spectroscopy and time-resolved photoluminescence measurements have been performed. Excitation of **BC1-BC2** in toluene at 510 nm (corresponding to a selective excitation of the **BC1** component at the Q_x band) resulted in immediate negative features centered at 509 nm and 713 nm, which correspond to ground-state bleaching of the **BC1** subunit (Figure 3, Table 2). These features decay with the concomitant rise of the negative feature at 527 nm and 760 nm, corresponding to ground-state bleaching of the **BC2** component of dyad. The time constant of decay of bleaching at 509 nm and 513 nm (τ_1 = 3.95 ± 0.13 ps) is the same as the time constant for the rise of bleaching at 527 nm and 760 nm. The same dynamics is observed upon excitation at 713 nm (corresponding to excitation of the **BC1** component at the Q_y band), in this case with corresponding time constant τ_1 = 3.59 ± 0.10 ps. In both cases, the ground-state bleaching of the **BC2** component decays subsequently with time constant τ_2 > 1.5 ns. Excitation of the dyad at 760 nm resulted in immediate formation of the ground state bleaching at 527 nm and 760 nm (no features corresponding to **BC1** component ground-state bleaching are observed), which subsequently decays with τ_2 > 1.5 ns (Figure S4). Analogous dynamics have been observed in PhCN, where the corresponding time constants for decay of ground-state bleaching of the **BC1** component and rise of ground-state bleaching of the **BC2** component are 2.55 ± 0.36 ps (for excitation at 510 nm) and 3.56 ± 0.12 ps (for excitation at 760 nm, Figures S3 and S4).

<Figure 3>

<Table 2>

The time constants for energy transfer can be calculated from the following equation:

$$k_{ET} = (\tau_{BC1\text{-}Dyad})^{-1} - (\tau_{BC1})^{-1}$$

where $\tau_{BC1\text{-}Dyad}$ is the excited state lifetime of the **BC1** component in dyad, and τ_{BC1} is the excited state lifetime of the **BC1** benchmark.

Taking an average τ_1 = 3.77 ± 0.16 ps, obtained from transient absorption spectroscopy as $\tau_{BC1\text{-}Dyad}$, and fluorescence lifetime of **BC1** τ_f = 5.82 ± 0.25 ns (Table 1) as τ_{BC1}, gives k_{ET} = (3.77 ± 0.06 ps)$^{-1}$ in toluene. Similar calculations gives k_{ET} = (3.06 ± 0.38 ps)$^{-1}$ in PhCN.

The k_{ET} for **BC1-BC2** is comparable with that obtained previously for chlorin-bacteriochlorin arrays [(4.8 ps)$^{-1}$] [21] and is substantially faster than that reported for weakly conjugated chlorin-chlorin arrays [(110 ps)$^{-1}$] [39]. This ultrafast energy transfer rate implies that the efficiency of energy transfer is > 0.99 in both solvents. To answer the question about the mechanism of the energy transfer, we calculated the rate of Förster energy transfer using the PhotochemCAD package [43,44]. These calculations required a precise knowledge of the interchromophoric distance R, since the rate of energy transfer decreases proportionally to $1/R^6$. The accurate distance determination between **BC1** and **BC2** subunits in dyad is challenging, due to a certain degree of conformational flexibility of the linker. In particular, two possible configurations on the amide function, *cis* and *trans* (Figure 4), lead to significantly different **BC1** – **BC2** distances. For the *trans* configuration, optimized by the AM1 method, the center-to-center distance between bacteriochlorins is calculated to be 22.13 Å, while for the *cis* configuration, the corresponding distance is 13.95 Å (Figure S5). Using these distances, the calculation for the *trans* isomer in toluene provides $k_{ET} = 1.5 \cdot 10^{10}$ s^{-1} [(65 ps)$^{-1}$] whereas for the *cis* isomer, $k_{ET} = 2.4 \cdot 10^{11}$ s^{-1} [4.1 ps)$^{-1}$] (see *Supplementary Information* for details). It is evident that, for the *trans* configuration, the calculated k_{ET} is an order of magnitude smaller than that determined experimentally, whereas, for the *cis* isomer, the calculated value matches very well the experimental value.

This results would suggest that the preferred conformation of the amide linker in dyad is *cis*, which is contrary to observations for simple amides, where *trans* stereoisomer is preferred [45]. DFT calculations indicate that the *cis* isomer of **BC1-BC2** is 17.9 kJ/mol higher in energy than *trans*-**BC1-BC2** (in vacuum). We therefore consider two alternative scenarios. First, it is in principle possible that the dyad undergoes *trans-cis* photoisomerization. However, we are not aware of any of prior studies reporting such isomerization, and TA data do not provide any indication for such a process. The second possibility is a through-bond mechanism (TB) for energy transfer. For the TB mechanism, electronic communication between energy donor and acceptor is essential [39]. The DFT calculations (Table S1) for **BC1-BC2** indicate that (1) corresponding molecular orbitals (MOs) are fully localized on each individual bacteriochlorin moiety, thus there is no orbital delocalization on both macrocycles; (2) there is negligible MO delocalization on the linker for HOMO, LUMO, HOMO-1, and LUMO-1 of either bacteriochlorin subunits. Such lack of delocalization is expected for the **BC1** subunit, because the phenyl linker is nearly perpendicular to the macrocycle plane (the DFT-calculated dihedral angle between phenyl and **BC1** rings is 72°). It is evident that there is very weak if any electronic communication between macrocycles. Therefore, it is reasonable to assume that the TB mechanism of energy transfer would be very inefficient.

The Förster mechanism in *cis* isomer thus appears to be the most likely mechanism to account for ultrafast energy transfer in **BC1-BC2**. It is possible that there are additional factors, such as solvation or intramolecular interactions,

which stabilize the *cis* conformation. More detailed computations and perhaps further spectroscopic studies are necessary to clarify this issue. Regardless of the exact mechanism, the energy transfer is very fast and efficient, which together with very moderate quenching of the excited state in polar solvents, is highly beneficial for potential application of amide-linked bacteriochlorin dyads.

<Figure 4>

SUMMARY

Bacteriochlorin-bacteriochlorin arrays with weakly conjugated amide linker were synthesized and characterized. The dyads feature two distinctive, narrow Q_y bands in the near-IR spectral window. Excitation of bacteriochlorin with the higher energy S_1 results in nearly quantitative and ultrafast energy transfer to the second dyad component. Both fluorescence quantum yield and excited state lifetime of the dyad is only moderately affected by the solvent polarity. This suggests that, contrary to strongly conjugated bacteriochlorin arrays, PET in the weakly conjugated dyad is negligible. Taken together, these properties make bacteriochlorin-bacteriochlorin arrays suitable for a variety of medical and energy-related applications.

EXPERIMENTAL

General. ^{1}H NMR spectra (400 MHz) and ^{13}C NMR (100 MHz) spectra were collected at room temperature in $CDCl_3$ unless noted otherwise. Chemical shifts (δ) were callibrated using residual solvent peaks (proton signals: 7.26 ppm for chloroform, 2.50 for DMSO, ^{13}C signals: 77.0 for chloroform, 39.5 ppm for DMSO). All solvents and commercialy available reagents were used as received. Commercially available anhydrous DMF was used without further purifications.

Absorption spectra were taken in toluene at room tempertature unless noted otherwise. Static emission spectra were taken in air-equilibrated toluene at room temperature in dilluted solution, with absorbance below 0.1. Quantum yields were determined in air-equilibrated solvents using tetraphenylporphyrin in air-equilibrated toluene (Φ = 0.070) [46] as a standard.

Transient absorption (TA) measurements were performed using a Helios spectrometer (Ultrafast Systems). Pump and probe laser pulses were derived from a regeneratively amplified Ti:Sapphire oscillator (Spectra Physics Tsunami/SpitfirePro) operating at 2 kHz. The pump pulse was passed to an optical parametric amplifier (OPA; Light Conversion TOPAS/NIRuVis) which was then selected to a have a wavelength corresponding to the specified absorption band of the array.

The samples for TA measurements were prepared by dissolving the array in toluene or PhCN such that the absorption bands being monitored have an optical density (OD) between 0.3 and 0.6. The prepared samples were placed in a 2-mm quartz cuvette which was housed in a thermoelectric temperature-controlled sample holder, and all

measurements were performed at 20°C. The sample were continuously stirred over the duration of the measurements to eliminate any thermal artifacts from the pump laser pulse. Pump laser pulse energies were set between 0.8μJ and 1.0μJ for all TA measurements. Analysis and fitting of the TA measurements were done using SurfaceXplorer (Ultrafast Systems); errors in the reported lifetimes correspond to errors obtained from the fits of the TA kinetics.

Time resolved photoluminescence (PL) measurements were performed by time-correlated single-photon counting (TCSPC). The samples were excited using a 510 nm pulsed diode laser (PicoQuant PDL 800-D) with a pulse width of approximately 150 nm. Individual photons were detected by an avalanche photodiode (MPD PDM Series) and the timing of the detected photons, referenced to the corresponding excitation pulse, was synchronized using timing electronics (PicoQuant PicoHarp 300). A histogram of the counts was then compiled over time and a least-squares fitting routine was performed to determine the lifetimes. Errors in the reported lifetimes correspond to the instrument response function (IRF).

Calculations.

Quantum mechanical calculations were performed and results were visualized using Spartan 10 for Windows (Wavefunction Inc, Irvine, CA). Structure optimization was performed using semi-empirical (AM1) or DFT using B3LYP functionals and 6-31G* basis sets in vacuum [47]. Full geometry optimization was performed. Förster energy transfer rates were calculated using PhotochemCAD software [43,44]. The following parameters were used for calculation of k_{ET}: extinction coefficient for maximum of acceptor absorption ε_{760} = 120,000 $M^{-1}{\cdot}cm^{-1}$, orientation factor κ^2 = 2/3, donor-acceptor distance R = 13.95 Å for *trans* isomer, and R = 13.95 Å for *cis* isomer. Donor-acceptor distances were obtained from AM1-optimized structures.

Synthesis. Known compounds **BC-Br** [42] and **BC2** [41] were synthesized following reported procedures. Compound **2** was reported previously [48] and synthesized here by a modified procedure.

BC-NH$_2$. A mixture of **BC-Br** (9.6 mg, 0.020 mmol), boronic ester **1** (42 mg, 0.20 mmol), and K_2CO_3 (27.0 mg, 0.20 mmol), in toluene/DMF (8 mL, 3:1) was degassed by freeze pump thaw cycles (3 times). A sample of $Pd(PPh_3)_4$ (4.6 mg, 0.0030 mmol) was added and the mixture was degassed once again by freeze pump thaw cycle. The resulting mixture was stirred under nitrogen at 100 °C overnight. The resulting mixture was diluted by ethyl acetate, washed (water, brine), dried (Na_2SO_4), and concentrated. Column chromatography provided a green solid (8.7 mg, 88%). ^{1}H NMR ($CDCl_3$, 400 MHz): δ -2.13 (b.s, 1H), -1.90 (b.s., 1H), 1.9 (s, 6H), 1.98 (s, 6H), 3.92 (bs, 2H), 4.08 (s, 2H), 4.42 (s, 1H), 4.51 (s, 1H), 7.00 (d, J = 8.2 Hz, 2H), 7.63 (d, J = 8.2 Hz, 2H), 8.22 (dd, J_1 =1.8 Hz, J_2 = 4.5 Hz, 1H), 8.64 dd, J_1 = 1.9 Hz, J_2 = 4.5 Hz, 1H), 8.66 (s, 1H), 8.69 (s, 1H), 8.70 dd, J_1 = 1.8 Hz, J_2 = 4.5 Hz, 1H), 8.92 dd, J_1 = 1.9 Hz, J_2 = 4.5 Hz, 1H). The resulting product was used in the next step without further characterization.

BC1-BC2. Following a procedure for synthesis of amide-linked chlorin-bacteriochlorin dyads [12], a mixture of BC2 (3.5 mg, 5.4 μmol), aqueous NaOH (1 mL, 1 M), THF (1 mL), and methanol (1 mL) was stirred at room

temperature for 16 hours. HCl solution (1 M, 5 mL) was added, and the resulting mixture was extracted with ethyl acetate. Combined organic layers were washed with brine, dried (Na_2SO_4), and concentrated. The resulting crude solid was suspended in DMF (1 mL), and treated with DMAP (2.6 mg, 54 μmol), BC-NH_2 (2.5 mg, 5.4 μmol) and EDCI (10.4 mg, 54 μmol). The resulting mixture was stirred at room temperature. After 16 hours, the mixture was diluted with ethyl acetate, washed with brine, dried (Na_2SO_4), and concentrated. A residue was purified with silica column chromatography (CH_2Cl_2) to afford a green-brown solid (BC1-BC2, 4.9 mg, 80%). ^{1}H NMR ($CDCl_3$, 400 MHz) δ: 8.96 (s, 1H), 8.94 (dd, J_1 = 1.8 Hz, J_2= 4.4 Hz, 1H), 8.86 (d, J = 1.8 Hz, 1H), 8.82 (d, J = 1.8 Hz, 1H), 8.72 (dd, J_1 = 1.8 Hz, = 4.4 Hz, 1H), 8.70 (s, 1H), 8.69 (s, 1H), 8.66 (dd, J_1 = 1.8 Hz, J_2 = 4.4 Hz, 1H), 8.60 (s, 1H), 8.56 (s, 1H), 8.25 (dd, J_1 = 1.8 Hz, J_2 = 4.4 Hz, 1H), 8.19 (s, 1H), 8.16 (d, J = 8.2 Hz, 2H), 8.07 (d, J = 8.2 Hz, 2H), 8.03 (d, J = 8.4 Hz, 2H), 7.91, (d, J = 8.4 Hz, 2H), 7.88-7.86 (m, 2H), 7.54-7.43 (m, 3H), 4.52 (s, 6H), 4.47 (s, 2H), 4.46 (s, 2H), 4.43 (s, 2H), 4.10 (s, 2H), 1.99 (s, 6H), 1.98 (s, 12H), 1.91 (s, 6H), -1.51 (bs, 1H), -1.77 (bs, 1H), -1.91 (bs, 1H), -2.17 (bs, 1H). MS ($[M]^+$, M = $C_{73}H_{67}N_9O_3$): Calcd: 1117.5362, Obsd: (HRMS-MALDI) 1117.5350.

N-(4-(4,4,5,5-tetramethyl-1,3,2-dioxaborolan-2-yl)phenyl)benzamide (**2**) [48]. A mixture of benzoic acid (183 mg, 1.50 mmol), 4-aminopheylboronic acid pinacol ester (219 mg, 1.00 mmol), DMAP (122 mg, 1.00 mmol), and EDC (286 mg, 1.50 mmol) in DMF (3 mL) was stirred at room temperature for 16 hours. The reaction mixture was diluted with ethyl acetate, washed (water and brine), dried (Na_2SO_4), and concentrated. The residue was purified by column chromatography [silica, hexane/ethyl acetate (3:1)] to afford product (174 mg, 54%). mp 239-240 °C; ^{1}H NMR ($CDCl_3$, 400 Hz): 7.90-7.86 (m, 2H), 7.85-7.819 (m, 3H), 7.67 (d, J = 8.2 Hz, 2H), 7.59-7.53 (m, 1H), 7.52-7.46 (m, 2H), 1.35 (s, 12H); ^{13}C NMR ($CDCl_3$, 100 MHz), 165.6, 140.6, 136.4, 135.9, 134.9, 131.9, 128.8, 127.0, 118.9, 83.7, 24.9; ESI-MS: Calcd: 323.1802, Obsd: 323.1797 ($[M+H]^+$, M = $C_{19}H_{22}BNO_3$); Anal. Calcd for $C_{19}H_{22}BNO_3$: C, 70.61; H, 6.86; N, 4.33. Found: C, 70.32; H, 6.75; N, 4.52.

BC1. A mixture of **BC-Br** (4.8 mg, 0.010 mmol), boronic ester **2** (6.5 mg, 0.020 mmol), and K_2CO_3 (13.8 mg, 0.100 mmol in toluene/DMF (3 mL, 2:1) was degassed by freeze pump thaw cycles and purged with nitrogen. A sample of $Pd(PPh_3)_4$ (3.5 mg, 0.003 mmol) was added under nitrogen, and the resulting mixture was further degassed by freeze pump thaw cycles and purged with nitrogen. The resulting mixture was stirred at 95-100 °C. After 21 hours, the reaction mixture was diluted with ethyl acetate, washed (water and brine), dried (Na_2SO_4), and concentrated. Column chromatography [hexane/ethyl acetate (5:1)] afforded BC1 as a green solid (4.9 mg, 82%). ^{1}H NMR ($CDCl_3$, 400 Hz), 8.94 (dd, J = 1.8, 4.3 Hz, 1H), 8.70 (dd, J = 1.8, 4.3 Hz, 1H)-8.68 (d, J = 4.1 Hz, 1H), 8.64 (dd, J = 1.8, 4.3 Hz, 1H), 8.22 (dd, J = 1.8, 4.3 Hz, 1H), 8.08 (s, 1H), 8.04-8.00 (m, 2H), 7.96 (d, J = 7.9 Hz, 2H), 7.87 (d, J = 8.6 Hz, 2H), 7.67-7.55 (m, 3H), 4.51 (s, 3H), 4.42 (s, 2H), 4.06 (s, 2H), 1.98 (s, 6H), 1.88 (s, 6H), -1.93 (s, 1 H), -2.19 (s, 1 H); ^{13}C NMR ($CDCl_3$, 100 MHz), 168.8, 168.6, 166.0, 158.9, 153.3, 139.1, 137.3, 137.1, 136.3, 135.5, 135.1, 135.0, 132.9, 132.0, 131.5, 129.0, 127.1, 122.9, 122.4, 120.8, 119.5, 117.4, 112.4, 97.4, 97.0, 65.2, 51.8, 47.5, 45.8, 45.2, 31.2, 31.0; ESI-MS: Calcd: 596.3026, Obsd: 596.3037 ($[M+H]^+$ M = $C_{38}H_{37}N_5O_2$).

Acknowledgement.

This work was supported by UMBC (start-up funds, SRAIS and START award) and partially by NSF (CHE-1955318 to M.Ptaszek). We thank Drs. Lisa Kelly and Steven J. Manning (UMBC) for their assistance in the initial lifetime measurements for **BC1**.

Supporting Information.

Additional spectra, details of the claculations, NMR spectra for new compounds.

REFERENCES

1. Fan, J, Hu M, Zhan P and Peng X. *Chem. Soc. Rev.* 2013; *42*, 29-43.
2. Wu L, Huang C, Emery BP, Sedgwick AC, Bull, He X-P, Tian H, Yoon J, Sessler JL and James TD. *Chem. Soc. Rev.* 2020; *49*, 5110-5139.
3. Peng H-Q, Niu L-Y, Chen Y-Z, Wu LZ, Tung C-H and Yang Q-Z. *Chem. Rev.* 2015; *115*, 7502-7542.
4. Ziessel R and Harriman A. *Chem. Comm.* 2011; *47*, 611-631.
5. El-Khouly ME, Fukuzumi S and D'Souza F. *ChemPhysChem* 2014, *15*, 30-47.
6. Ultrafast Photoinduced Energy and Charge Transfer. *Faraday Discuss.* 2019, *38*, *whole issue dedicated to energy and charge transfer in multichromophoric arrays*.
7. Lindsey JS. *Chem. Rev.* 2015; *115*, 6534-6620.
8. Taniguchi M and Lindsey JS. *Chem. Rev.* 2017; *117*, 344-535.
9. Brückner C, Samankumara L and Ogikubo J. *in Handbook of Porphyrin Sciences,* Kadish, K. M.; Smith, K. M.; Guilard, R., (Eds). World Scientific: River Edge, NY, 2012, vol. 17, pp 1-112.
10. Lindsey J, Mass O and Chen C-Y. *New J. Chem.* 2011; *35*, 511-516.
11. Kee HL, Nothdurft R, Muthiah C, Diers JR, Fan D, Ptaszek M, Bocian DF, Lindsey JS, Culver JP and Holten, D. *Photochem. Photobiol.* 2008; *84*, 1061-1072.
12. Ogata F, Nagaya T, Maruoka Y, Akhigbe J, Meares A, Lucero M, Satraitis A, Fujimura D, Okada R, Inagaki F, Choyke P, Ptaszek M and Kobayashi H. *Bioconjugate Chem.* 2019; *30*, 169-183.
13. Ng, K. K.; Takada, M.; Jin, C. C. S.; Zheng, G. Self-Sensing Porphysome for Fluorescence-Guided Photothermal Therapy. *Bioconjugate Chem.* 2015, *26*, 345-351.
14. Yang E, Kirmaier C, Krayer M, Taniguchi M, Kim H-J, Diers JR, Bocian DF, Lindsey JS and Holten D. *J. Phys. Chem. B.* 2011; *115*, 10801-10816.
15. Blankenship RE. *Molecular Mechanisms of Photosynthesis*; John Wiley & Sons, 2014.
16. Yu Z and Ptaszek M. *J. Org. Chem.* 2013; *78*, 10678-10691.
17. Taniguchi M, Cramer DL, Bhise AD, Kee, HL, Bocian DF, Holten D and Lindsey JS. *New J. Chem.* 2008; *32*, 947–958.
18. Kataoka Y, Shibata Y and Tamiaki H. *Chem. Lett.* 2010; *39*, 953-955.

19. Osuka A, Wada Y, Maruyama K and Tamiaki H. *Heterocycles,* 1997; *44*, 165.
20. Grin MA. Lonin IS. Fedyunin SV, Tsiprovskiy AG, Strizhakov AA, Tsygankov AA., Krasnovsky AA and Mironov, AF. *Mendeleev Commun.* 2007; *17*, 209-211.
21. Muthiah C, Kee HL, Diers JR, Fan D, Ptaszek M, Bocian DF, Holten, D and Lindsey JS. *Photochem. Photobiol.* 2008; *84*, 786-801.
22. Kee HL, Diers JR, Ptaszek M, Muthiah C, Fan D, Lindsey JS, Bocian DF and Holten D. *Photochem. Photobiol.* 2009; *85*, 909-920.
23. Esemoton NN, Satraitis A, Wiratan L and Ptaszek M. *Inorg. Chem.* 2018; *57*, 2977-2988.
24. Dukh M, Tabaczynski WA, Seetharaman S, Ou Z, Kadish KM, D'Souza F and Pandey RK *Chem. Eur. J.* 2020, *26*, 14996-15006.
25. Wasielewski MR and Svec WA. *J. Org. Chem.* 1980; *45*, 1969-1974.
26. Yu Z, Pancholi C, Bhagavathy GV, Kang HS, Nguyen JK and Ptaszek, M. *J. Org. Chem.* 2014; *79*, 7910-7925.
27. Kang HS, Esemoto NN, Diers J, Niedzwiedzki D, Greco J, Akhigbe J, Yu Z, Pancholi C, Viswanathan BG, Nguyen JK, Kirmaier C, Birge R, Ptaszek M, Holten D and Bocian DF. *J. Phys. Chem. A* 2016; *120*, 379-385.
28. Nopondo EN, Yu Z, Wiratan L, Satraitis A and Ptaszek M. *Org. Lett.* 2016; *18*, 4590-4593.
29. McLeese C, Yu Z, Esemoto NN, Kolodziej C, Maiti B, Bhandari S, Dunietz BD, Burda C and Ptaszek M. *J. Phys. Chem. B*, 2018; *122*, 4131-4140.
30. Meares A, Yu Z, Bhagavathy GV, Satraitis A and Ptaszek M. *J. Org. Chem.* 2019; *84*, 7851- 7862.
31. Uthe B, Meares A, Ptaszek M and Pelton M. *J. Chem. Phys.* 2020; *153*, 074302.
32. Meares A, Satraitis A and Ptaszek M. *J. Org. Chem.* 2017; *82*, 13068-13075.
33. Meares A, Satraitis A, Akhigbe J, Santhanam N, Swaminathan S, Ehudin M and Ptaszek M. *J. Org. Chem.* 2017; *82*, 6054-6070.
34. Grin MA, Toukach PV, Tsvetkov VB, Reshetnikov RI., Kharitonova OV, Kozlov AS, Krasnovsky AA and Mironov A. F. *Dyes and Pigments*, 2015; *212*, 21-29.
35. Hu G, Liu R, Alexy EJ, Mandal AK, Bocian DF, Holten D and Lindsey JS. *New. J. Chem.* 2016; *40*, 8032-8052.
36. Panchenko PA, Sergeeva AN, Fedorova OA, Fedorov YV, Reshetnikov RI, Schelkunova AE, Grin MA, Mironov AF and Jonusauskas G. *J. Photochem. Photobiol. B*, 2014; *133*, 140-144.
37 Ponsot F, Desbois N, Bucher L, Berthelot M, Mondal P, Gros CP and Romieu A. *Dyes and Pigments*, 2019; *160*, 747-756.
38. Ponsot F, Bucher L, Desbois N, Rousselin Y, Mondal P, Devillers CH, Romieu A, Giros CP, Singhal R and Sharma GD. *J. Mater. Chem. C*, 2019; *7*, 9655-9664.
39. Holten D, Bocian DF and Lindsey JS. *Acc. Chem. Res.* 2002; *35*, 57-69.
40. Taniguchi M, Ra D, Kirmaier C, Hindin E, Schwartz JK, Diers JR, Knox RS, Bocian DF, Lindsey JS and Holten D. *J. Am. Chem. Soc.* 2003; *125*, 13461–13470.

41. Yu Z and Ptaszek M. *Org. Lett.* 2012; *14*, 3708-3711.

42. Krayer M. Ptaszek M, Kim H-J, Meneely KR, Fan D, Secor K and Lindsey JS. *J. Org. Chem.* 2010; *75*, 1016-1039.

43. Du H, Fuh RCA, Li JZ, Corkoran LA and Lindsey JS. *Photochem. Photobiol.* 1998; *68*, 141-142.

44. Taniguchi M, Du H and Lindsey JS. *Photochem. Photobiol.* 2018; *94*, 277-289.

45. Eliel EL, Wilen SH. Stereochemistry of Organic Compounds, 1994, John Wiley and Sons.

46. Mandal AK, Taniguchi M, Diers JR, Niedzwiedzki DM, Kirmaier C, Lindsey JS, Bocian DF and Holten D. *J. Phys. Chem. A,* 2016; *120*, 9719-9731.

47. Except for molecular mechanics and semi-empirical methods, the calculation methods used in Spartan ′10 have been documented in: Shao Y, Molnar LF, Jung Y, Kussmann J. Ochsenfeld C, Brown ST, Gilbert ATB, Slipchenko LV, Levchenko SV, O'Neill DP, DiStasio RA Jr, Lochan RC, Wang T, Beran GJO Besley NA, Herbert JM, Lin CY, Van Voorhis T, Chien SH, Sodt A, Steele RP, Rassolov VA, Maslen PE, Korambath PP, Adamson RD, Austin B, Baker J, Byrd EFC, Dachsel H, Doerksen RJ, Dreuw A, Dunietz BD, Dutoi AD, Furlani TR, Gwaltney SR, Heyden A, Hirata S, Hsu CP, Kedziora G, Khalliulin RZ, Klunzinger P, Lee AM, Lee MS, Liang WZ, Lotan I, Nair N, Peters B, Proynov EI, Pieniazek PA, Rhee YM, Ritchie J, Rosta E, Sherrill CD, Simmonett AC, Subotnik JE, Woodcock HL III, Zhang W, Bell AT, Chakraborty AK, Chipman DM, Keil FJ, Warshel A, Hehre WJ, Schaefer HF III, Kong J, Krylov AI, Gill PMW and Head-Gordon M. *Phys. Chem. Chem. Phys.* 2006; *8*: 3172–3191.

48. Dai Y, Hartandi K, Ji Z, Ahmed AA, Albert DH, Bauch JL, Bouska JJ, Bousquet PF, Cunha GA, Glaser KB, Harris CM, Hickman D, Guo J, Li J, Marcotte PA, Marsh KC, Moskey MD, Martin RL, Olson AM, Osterling DJ, Pease LJ, Soni NB, Stewart KD, Stoll VS, Tapang P, Reuter DR, Davidsen SK and Michaelides MR. *J. Med. Chem.* 2007; *50*, 1584-1597.

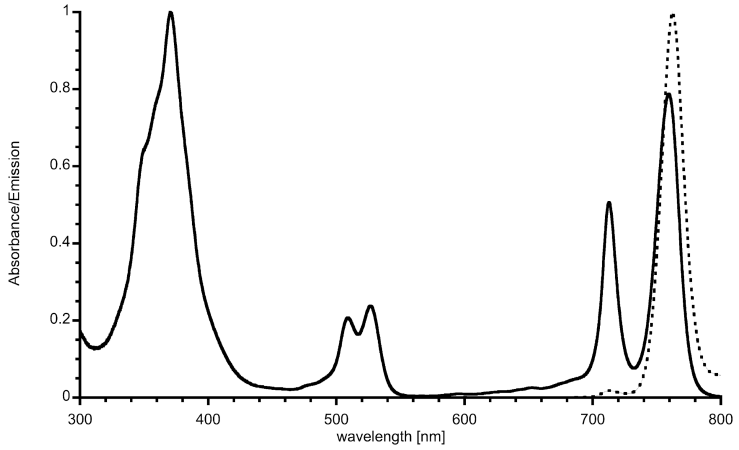

Figure 1. Absorption (solid) and emission (dotted) spectra of **BC1-BC2** in toluene (excitation wavelength for emission spectra λ_{exc} = 509 nm).

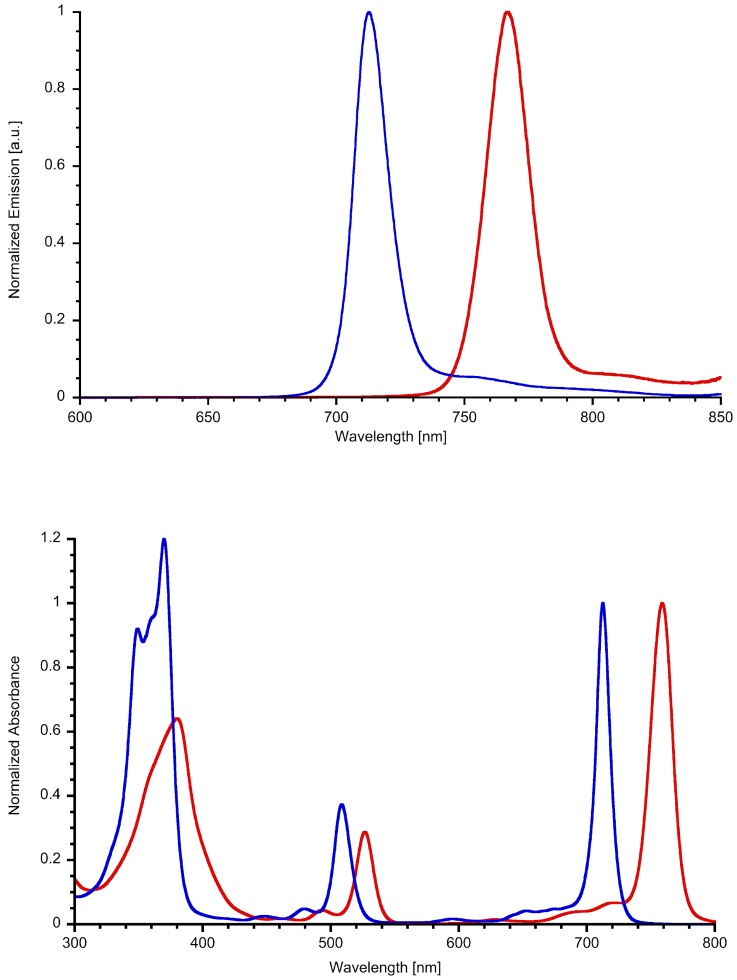

Figure 2. Absorption (lower panel) and emission (upper panel) of **BC1** (blue) and **BC2** (red) in toluene. Sample were excited at the maxima of the Q_x bands.

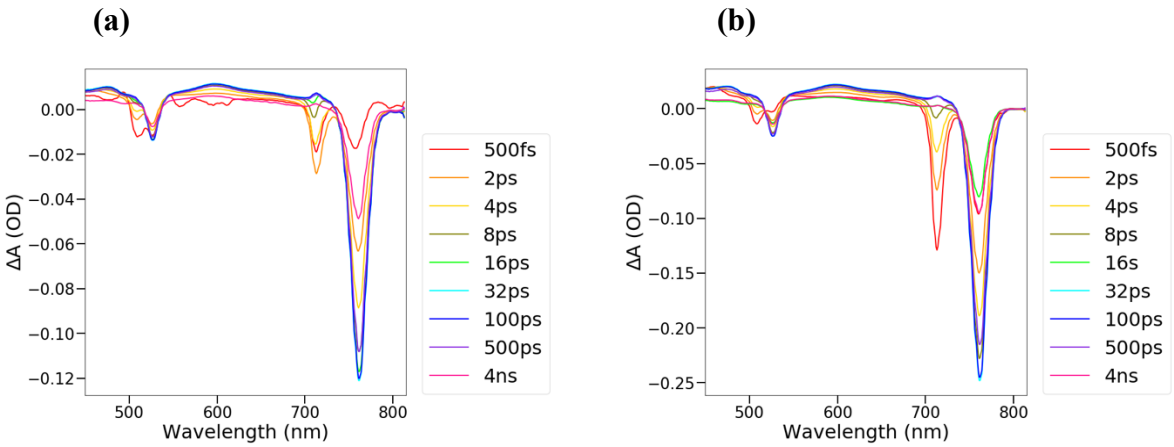

Figure 3. Transient absorption spectra for different pump-probe delay for **BC1-BC2** in toluene. Pump wavelength 510 nm (a) and 713 nm (b).

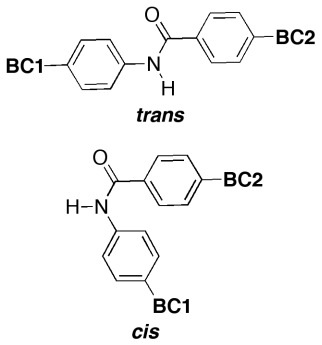

Figure 4. Schematic representation of *trans* and *cis* configuration of **BC1-BC2** dyad.

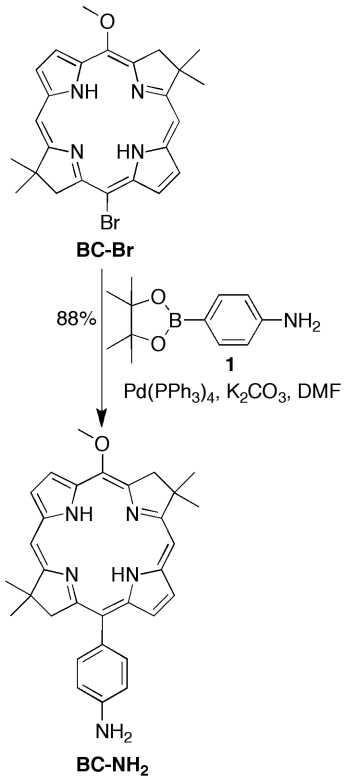

Scheme 1. Synthesis of 4-aminophenyl-substituted building block **BC-NH_2.**

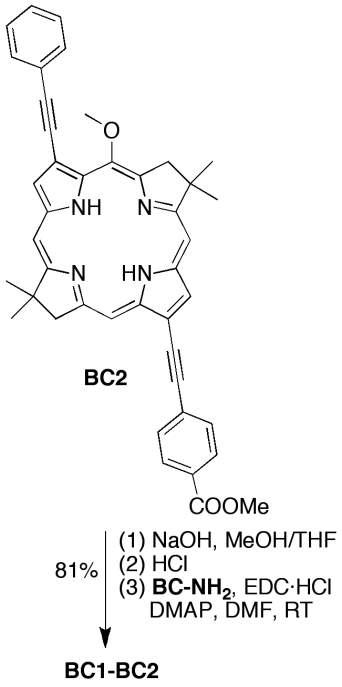

Scheme 2. Synthesis of dyad **BC1-BC2**.

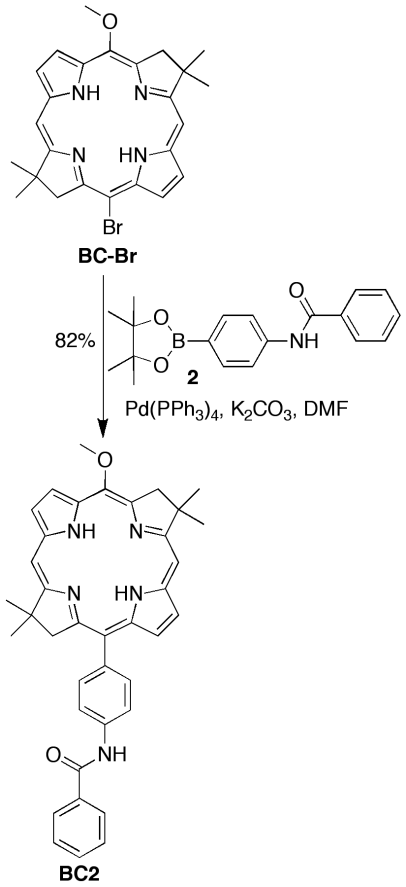

Scheme 3. Synthesis of benchmark monomer **BC1**.

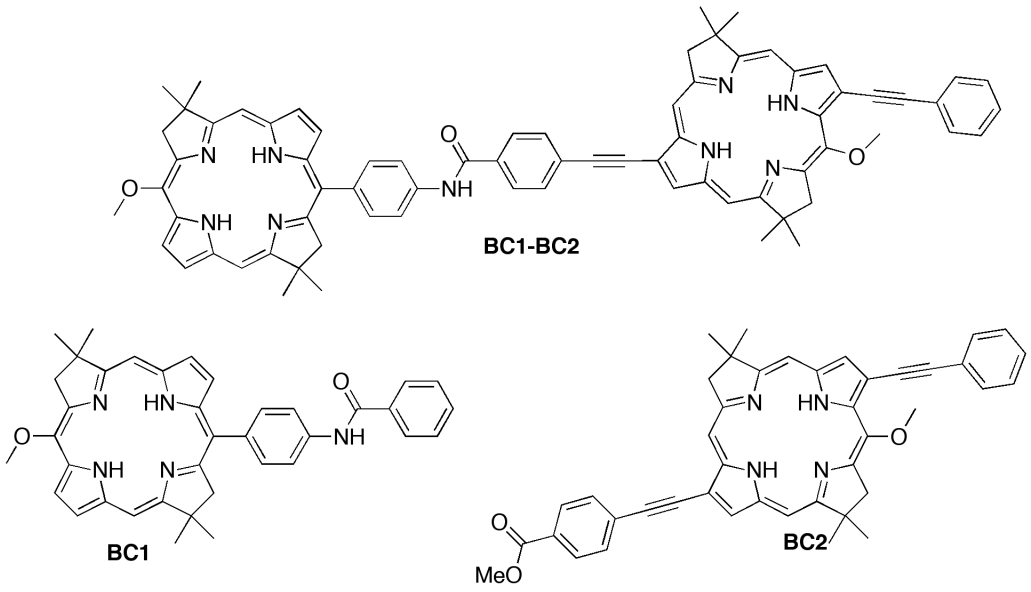

Chart 1. Structure of bacteriochlorin0bacteriochlorin dyad **BC1-BC2** and benchmark monomers **BC1** and **BC2**.

Table 1. Absorption and emission data for the dyad **BC1-BC2** dyad and benchmark monomers **BC1** and **BC2**. All data in toluene, unless noted otherwise.

Compound	*B* [nm]	Q_x [nm]	Q_y [nm]	λ_{em} [nm]	Φ_f	τ_f [ns]
BC1-BC2	370	509, 526	713, 760	762	0.24 (0.19[b])	4.37 ± 0.25 (3.58 ± 0.25[b])
BC1	349, 370	509	713	713	0.19 (0.18[b])	5.82 ± 0.25 (5.29 ± 0.25[a])
BC2	380	527	760	763	0.23 (0.23[a])	4.16 ± 0.25 (4.30 ± 0.25[a])

a Data in PhCN. *b* Data in DMF.

Table 2. TA data for **BC1-BC2**

Pump wavelength	τ_1 (toluene)	τ_1 (PhCN)	τ_2 (toluene)	τ_2 (PhCN)	k_{ET} (toluene)	k_{ET} (PhCN)
510 nm	3.95±0.13 ps	2.55±0.36 ps	> 1.5 ns	> 1.5 ns	(3.77 ± 0.06 ps)$^{-1}$	(3.06 ± 0.38 ps)$^{-1}$
713 nm	3.59±0.01 ps	3.56±0.12 ps	> 1.5 ns	> 1.5 ns		
760 nm	-	-	> 1.5 ns	> 1.5 ns		

τ_1 – time constant for decay of bleaching at 713 nm and rise the bleaching at 760 nm

τ_2 – time constant for decay of bleaching at 760 nm